Analysis of Optically Controlled Microwave/Millimeter-Wave Device Structures

RAINEE N. SIMONS, MEMBER, IEEE, AND KUL B. BHASIN, MEMBER, IEEE

Abstract—**Light-induced voltage and the change in the source-to-drain channel current under optical illumination higher than the semiconductor band gap for GaAs MESFET, InP MESFET, $Al_{0.3}Ga_{0.7}As$/GaAs high electron mobility transistor (HEMT), and GaAs permeable base transistor (PBT) are analytically obtained. The GaAs PBT and GaAs MESFET have higher sensitivity than the InP MESFET. However, the $Al_{0.3}Ga_{0.7}As$/GaAs HEMT is observed to have the highest sensitivity.**

Variations in the small-signal parameters, such as channel conductance, gate-to-source capacitance, and transconductance, as well as transient parameters, such as switching time and power–delay product, of GaAs MESFET with illumination are computed. The computed capacitance and transconductance are compared with the experimentally obtained values and are found to be in fair agreement. Based on these results, the design considerations for an optically controlled MESFET switch are discussed. Finally, variation in device parameter due to optical illumination and its effect on the cutoff frequencies f_T and f_{max} are also investigated.

I. Introduction

DIRECT OPTICAL CONTROL of microwave devices and monolithic microwave integrated circuits (MMIC's) can result in better switching, amplitude, phase control, and frequency control [1]. It allows the use of optical fiber technology for interconnection of microwave devices and circuits, thereby reducing crosstalk and electromagnetic interference. It can also reduce weight, enhance efficiency, and increase the speed of operation of microwave systems [2]. Furthermore, in the case of III–V compound semicondutor devices and circuits, the optical absorption coefficient and energy band gap can be tailored to a particular wavelength by adjusting the mole fraction (x) of its constituents [3]. Besides, the III–V compound semiconductor devices can be integrated with other MMIC components on a single semi-insulating GaAs or InP substrate [4]. These offer further advantages for direct optical control of microwave devices and circuits in microwave systems.

Several authors have experimentally investigated the effect of optical illumination on the drain characteristics, the gate-to-source capacitance, the transconductance, and the scattering parameters of GaAs metal–semiconductor field-effect transistor MESFET's [5]–[9]. However, the effect of illumination on the small-signal parameters and the transient parameters has not been fully investigated. Besides, the effect of optical illumination on other III–V compound semiconductor field-effect transistors, such as InP MESFET, $Al_xGa_{1-x}As$/GaAs high electron mobility transistor (HEMT), and the permeable base transistor (PBT), for microwave and millimeter-wave applications has not been considered.

In this paper, we investigate the effect of light on several III–V compound semiconductor devices, such as GaAs MESFET, InP MESFET, $Al_xGa_{1-x}As$/GaAs HEMT, and GaAs PBT. The computed results illustrate a) the light-induced voltage as a function of the incident optical power density; b) the change in the drain current with change in optical power density as a function of the drain-to-source voltage; and c) the variation in the small-signal parameters, such as channel conductance, gate-to-source capacitance, and transconductance, and in transient parameters, such as switching time and power-delay product, of GaAs MESFET with illumination. The computed gate-to-source capacitance and transconductance are compared with the experimentally measured values for GaAs MESFET. Based on these results, the design aspects of an optically controlled MESFET switch are discussed. Besides, its equivalent circuit parameters under switching conditions are computed and the figure of merit is determined.

Finally, the variation in the device parasitics due to optical illumination, and its effect on the cutoff frequencies f_T and f_{max} are qualitatively discussed.

II. Light-Induced Voltage

The operation of these microwave devices as photodetectors and amplifiers depends on the photo-generation of electron–hole pairs in their active layer. Fig. 1 illustrates several techniques for direct optical control of microwave solid-state devices. In these techniques, light from a laser [10], a light-emitting diode (LED) [11], or an optical waveguide [12] is incident on the active layer of the device. The incident optical power increases the concentration of the minority carriers, for example, the holes in a n-type channel. This increase in hole concentration Δp is proportional to αd if $\alpha d \ll 1$. Mathematically, Δp is expressed as [13], [14]

$$\Delta p = \frac{\tau}{d}\left[\frac{P_{opt}\lambda}{hc}\right](1 - e^{-\alpha d}) \quad (1)$$

Manuscript received March 20, 1986; revised July 9, 1986.

The authors are with the NASA Lewis Research Center, Cleveland, OH 44135.

IEEE Log Number 8610830.

0018-9480/86/1200-1349$01.00 ©1986 IEEE

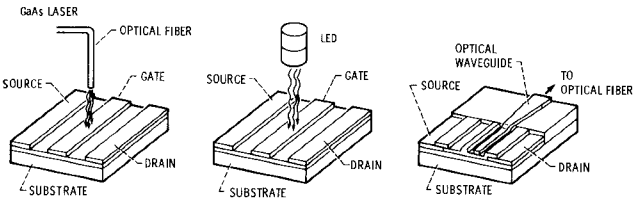

Fig. 1. Proposed techniques for direct optical control of microwave devices. (a) Optical fiber illuminating a MESFET. (b) LED illuminating a MESFET. (c) Optical waveguide coupling light to a MESFET.

where h is Planck's constant, P_{opt} is the incident optical power per unit area (and is the same as P in all the figures), λ is the wavelength of the incident light, α is the optical absorption coefficient of the semiconductor, d is the thickness of the active layer, τ is the minority carrier lifetime, and c is the speed of light in vacuum. The quantity inside the square brackets represents the number of photons of wavelength λ incident on a unit area per second.

The light-induced voltage V_{lit} is expressed as [13], [14]

$$V_{lit} = \frac{kT}{q} \ln\left(\frac{p+\Delta p}{p}\right) \tag{2}$$

where k is Boltzmann's constant, T is the temperature in degrees Kelvin, and q is the electronic charge. The variable p is the equilibrium minority carrier concentration in the active layer, for example, holes in a n-type channel, and is given by [13]

$$p = \frac{n_i^2}{n} \tag{3}$$

where n_i is the intrinsic carrier concentration, and n is the carrier concentration (and is the same as N_D in all the figures).

III. Effect of Light on the Drain Characteristics, Channel Conductance, Gate-To-Source Capacitance, Transconductance, Switching Time, and Power–Delay Product of GaAs and InP MESFET's

The drain current I_{ds} as a function of the applied gate bias voltage V_{gs} and the drain-to-source voltage V_{ds} for a MESFET is expressed as [13], [14]

$$I_{ds} = \frac{q\mu nWd}{l}\left[V_{ds} - \frac{2}{3}\frac{1}{V_p^{1/2}}\left\{\left(V_{ds}+V_b-V_{gs}\right)^{3/2} - \left(V_b-V_{gs}\right)^{3/2}\right\}\right] \tag{4}$$

where μ is the electron mobility, W and l are the gate width and length, respectively, V_b is the built-in Schottky barrier voltage, and V_p is the pinchoff voltage required to completely deplete the active layer. V_p is given by [13]

$$V_p = \frac{qnd^2}{2\epsilon_0\epsilon_r} \tag{5}$$

where ϵ_0 is the permittivity in vacuum and ϵ_r is the relative permittivity of the active layer. Illuminating the MESFET is equivalent to forward biasing the gate of the MESFET by a voltage source equal to V_{lit}. The net voltage at the gate is therefore a superposition of the gate bias V_{gs} and V_{lit}. The drain conductance g_d is given by [15], [16]

$$g_d \simeq \frac{q\mu nWd}{l}\left[1-\left(\frac{V_b-V_{gs}}{V_p}\right)^{1/2}\right]. \tag{6}$$

The gate-to-source and drain-to-gate capacitances C_{gs} and C_{dg} are given by [15], [16]

$$C_{gs} \simeq C_{dg} \simeq \frac{Wl}{2\sqrt{2}}\left(\frac{qn\epsilon_0\epsilon_r}{V_b-V_{gs}}\right)^{1/2}. \tag{7}$$

The transconductance g_m in the saturation region is given by [15], [16]

$$g_m \simeq \left[\frac{qn\epsilon_0\epsilon_r}{2\left(V_b-V_{gs}\right)}\right]^{1/2} V_s W \tag{8}$$

where V_s is the saturation electron drift velocity. The assumption that is made while deriving the above equations is that the current saturation occurs when the average electric field under the gate reaches the domain-sustaining field

$$E_s = \frac{V_s}{\mu}. \tag{9}$$

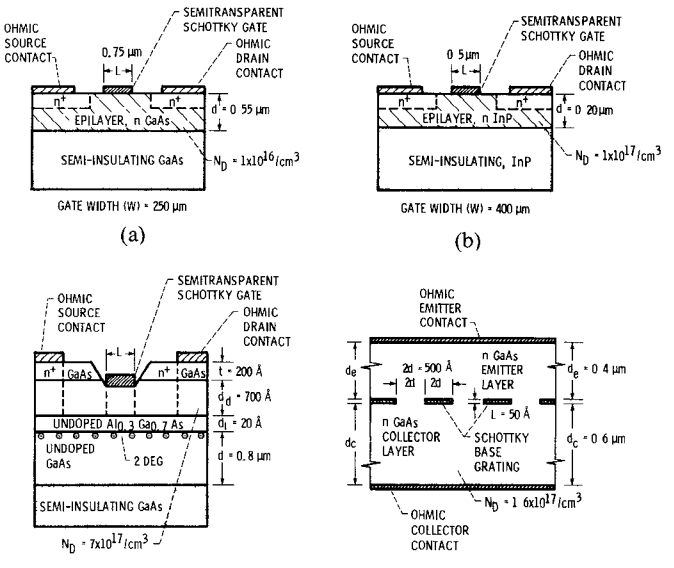

Fig. 2. Cross-sectional view with material parameters of various microwave device structures for direct optical control of monlithic microwave and millimeter-wave integrated circuits. (a) GaAs MESFET. (b) InP MESFET. (c) AlGaAs/GaAs HEMT. (d) GaAs PBT.

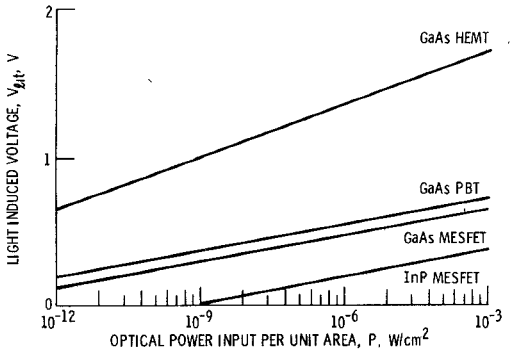

Fig. 3. Computed light-induced voltage versus the incident optical power for various microwave device structures.

The switching time τ is expressed as [15], [16]

$$\tau = \frac{l}{V_s} \frac{(V_b - V_{gs})^{1/2}}{\left[V_p^{1/2} - (V_b - V_{gs})^{1/2}\right]}. \quad (10)$$

Finally, the power–delay product is equal to [15], [16]

$$P\tau = Wl^2 E_s \left[2\epsilon_0 \epsilon_r qn(V_b - V_{gs})\right]^{1/2}. \quad (11)$$

IV. Effect of Light on the Drain Characteristics of $Al_{0.3}Ga_{0.7}As$/GaAs HEMT

The drain current I_{ds} for a depletion-mode (normally-ON) HEMT is expressed as [17]

$$I_{ds} = \left(37.8V_{gs} - 158V_{gs}^2 - 360V_{gs}^3 + 18.5\right) \cdot \tan^{-1}\left[\frac{V_{ds}}{0.07 + 0.1V_{gs}} + 0.25V_{ds}\right] \quad (12)$$

and for an enhancement-mode (normally-OFF) HEMT is expressed as [17]

$$I_{ds} = (49.8V_{gs} - 13.64) \times \tan^{-1}\left[\frac{V_{ds}}{0.143V_{gs}} + 0.5V_{ds}\right]. \quad (13)$$

The net voltage at the gate is a superposition of V_{gs} and V_{lit}.

V. Computed Results and Discussions

A. Light Sensitivity

The thickness of the active layer, the gate width and length, and the doping density are presented in Fig. 2 for GaAs MESFET, InP MESFET, $Al_{0.3}Ga_{0.7}As$/GaAs HEMT, and GaAs PBT. The properties of the semiconductors used in the fabrication of these microwave devices are presented in Table I. The computed light-induced voltage using (2) is presented in Fig. 3 as a function of the incident optical power density for the devices shown in Fig. 2. The light-induced voltage increases linearly with the incident optical power. At a fixed incident optical power density, the $Al_{0.3}Ga_{0.7}As$/GaAs HEMT has the highest sensitivity and the InP MESFET the lowest sensitivity. The sensitivities of GaAs PBT and GaAs MESFET are almost identical and fall midway between those of HEMT and InP MESFET.

TABLE I
Properties of Semiconductors Used in the Fabrication of Microwave Devices at 300 K

Material	Electron Mobility μ, cm^2/V sec	Intrinsic Carrier Concentration n_i, cm^{-3}	Optical Absorption Coefficient α, cm^{-1}	Wave Length λ, μm	Minority Carrier Lifetime τ, sec	Relative Permittivity, ϵ_r	Schottky Barrier Voltage, V_b
GaAs	5300	1.78×10^6	1.00×10^4	0.87	1×10^{-8}	13.1	GOLD:0.9 ITO:0.95
InP	3300	1.97×10^9	1.80×10^4	1.06	1.10^{-8}	12.55	GOLD:0.5
$Al_{0.3}Ga_{0.7}As$	9000	2.5×10^3	1.25×10^4	0.653	2×10^{-8}	12.2	GOLD:1.11

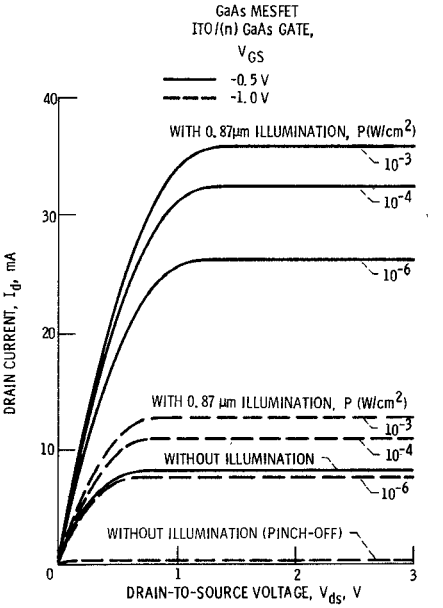

Fig. 4. Computed drain current versus the drain-to-source voltage for GaAs MESFET with ITO/(n) GaAs Schottky gate for various incident optical power levels.

B. GaAs MESFET Drain Characteristics Under Illumination

The gate metallization in a conventional MESFET is gold; hence, the gate is not transparent to light. This limitation can be overcome if the gate metallization is indium tin oxide. Indium tin oxide is transparent to visible light [18] and also forms a good Schottky contact with GaAs [19]. The computed drain characteristics using (4) for a GaAs MESFET with indium tin oxide gate are shown in Fig. 4. In Fig. 5, the ratio of the saturation drain current with and without illumination as a function of the gate-to-source voltage at a fixed incident optical power density of 1 μW/cm^2 for a GaAs MESFET is shown. From this figure, it is observed that the optical gain of a normally-OFF MESFET is a maximum if the gate-to-source bias is such that the MESFET is in pinchoff condition.

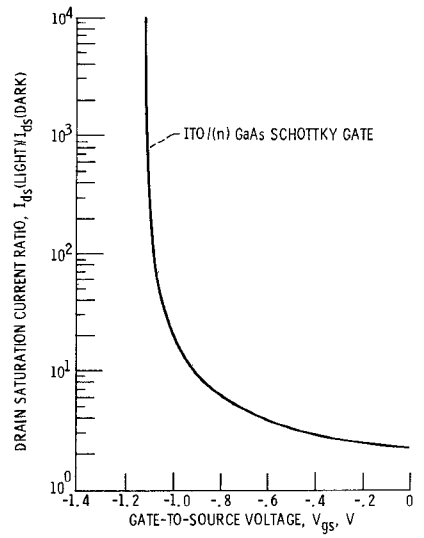

Fig. 5. Computed ratio of drain saturation current with and without illumination versus the gate voltage for a GaAs MESFET. The incident optical power level is kept constant at 1 $\mu W/cm^2$.

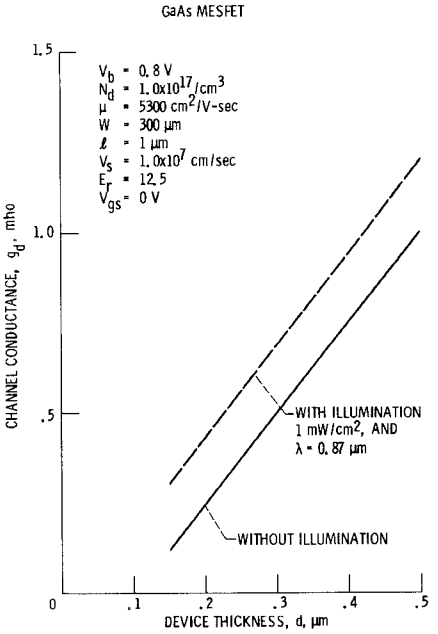

Fig. 6. Computed channel conductance versus device active layer thickness.

C. GaAs MESFET Small-Signal and Transient Parameters Under Illumination

Equation (6) is used for computing the channel conductance g_d with and without illumination. The computed results are illustrated in Fig. 6, which shows that the channel conductance increases by about 15 percent under illumination. Computations by DeSalles and Forest [20] show a 10-percent decrease in the parasitic series resistance at the ends of the channel under illumination, which is in fair agreement with our results.

Equation (7) is used for computing the gate-to-source and drain-to-gate capacitance C_{gs} and C_{dg} with and also without illumination. The computed gate-to-source capacitance C_{gs} is compared with the experimentally measured

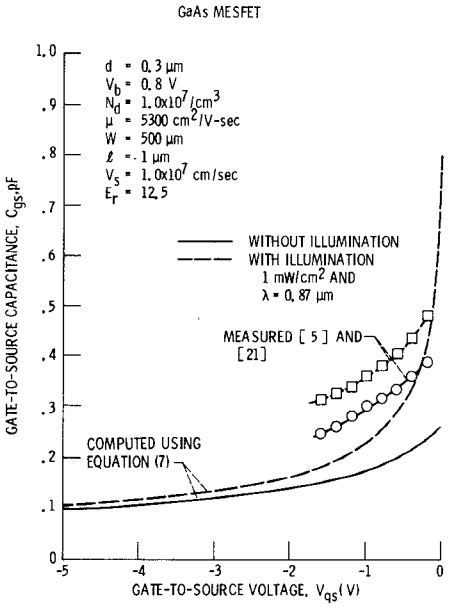

Fig. 7. Computed and measured gate-to-source capacitance versus the gate-to-source voltage.

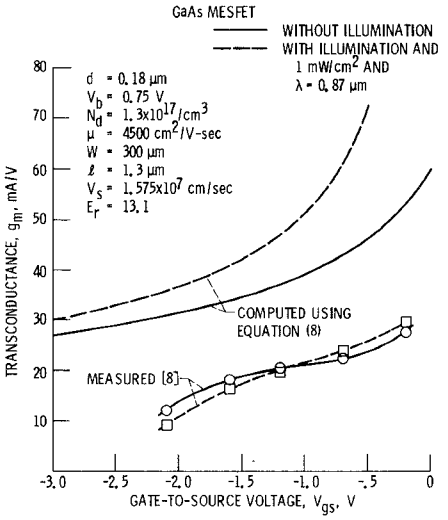

Fig. 8. Computed and measured dc transconductance versus the gate-to-source voltage.

values of C_{gs} in Fig. 7. The experimentally measured values of C_{gs} are taken from Sun *et al.* [5], [21]. Equation (8) is used for computing the dc transconductance g_m with and also without illumination. The computed dc g_m is compared with the experimentally determined values in Fig. 8. The experimentally determined values of *dc* g_m are taken from Gautier *et al.* [8]. The discrepancy between the computed and the measured values of C_{gs} and g_m is due to the fact that the simple analytical model used in predicting their values is based on assumptions [15], [16] which may not be fully justified in the above case. However, the model requires very small computer time as compared to a rigorous two-dimensional numerical technique. The crossover observed in the experimental plot of C_{gs} has been explained in [8].

Switching time τ with and without illumination is computed using (10) as a function of the device active

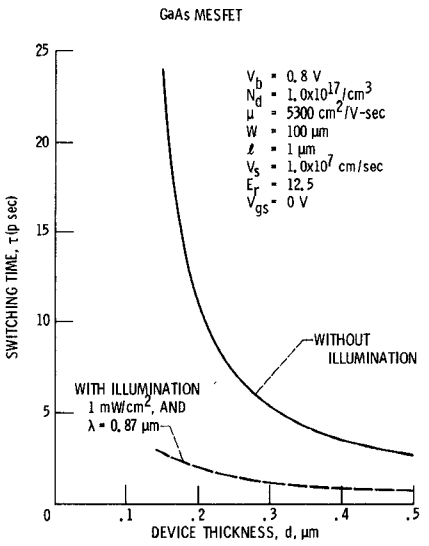

Fig. 9. Computed switching time versus the active layer thickness.

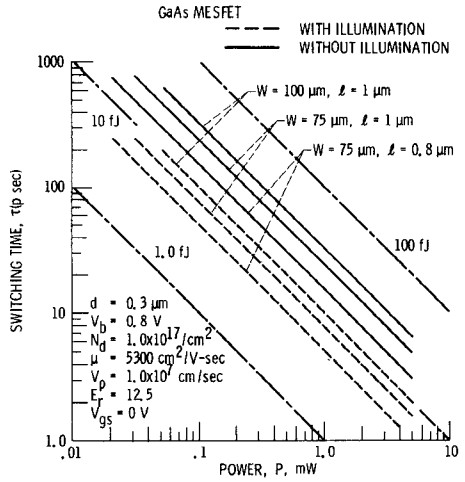

Fig. 10. Computed switching time versus the power.

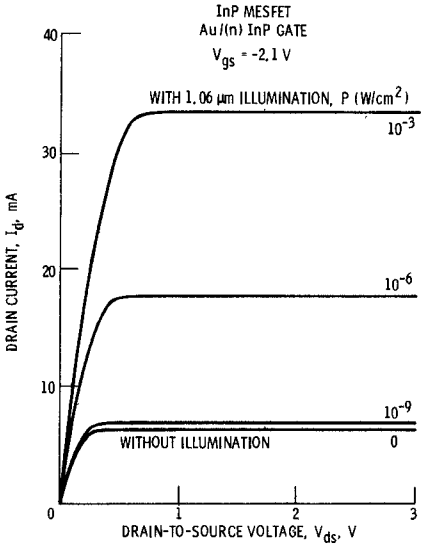

Fig. 11. Computed drain current versus the drain-to-source voltage for InP MESFET with Au/(n) InP Schottky gate for various incident optical power levels.

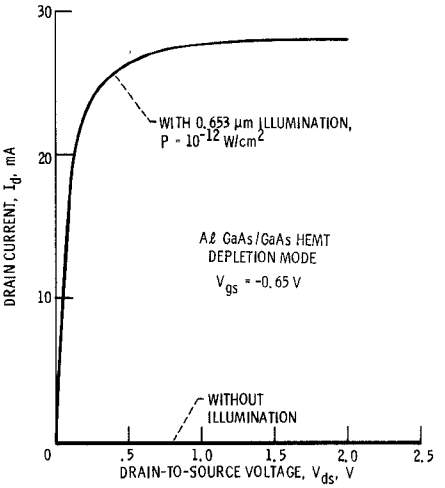

Fig. 12. Computed drain current versus the drain-to-source voltage of a depletion-mode (normally-ON) AlGaAs/GaAs HEMT.

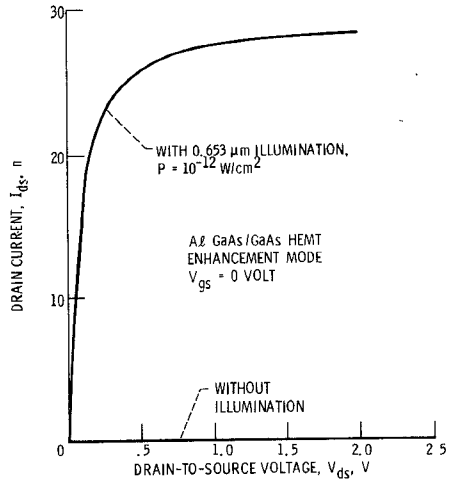

Fig. 13. Computed drain current versus the drain-to-source voltage of an enhancement-mode (normally-OFF) AlGaAs/GaAs HEMT.

layer thickness (Fig. 9) and also as a function of the gate power dissipation (Fig. 10). In Fig. 10, the constant power–delay product $P\tau$ in femtojoules is indicated by a dash-and-dot line. From Figs. 9 and 10, it is observed that illumination improves the switching time and lowers the switching energy. It may also be mentioned that our observations are in agreement with the qualitative discussions by Goronkin *et al.* [22] regarding the effect of light on the switching time and switching energy.

D. InP MESFET Drain Characteristic Under Illumination

The drain current characteristic of a InP MESFET computed using (4) is shown in Fig. 11.

E. $Al_{0.3}Ga_{0.7}As/GaAs$ HEMT Drain Characteristic Under Illumination

The drain current characteristics of a depletion-mode and an enhancement-mode $Al_{0.3}Ga_{0.7}As/GaAs$ HEMT computed using (12) and (13) are shown in Figs. 12 and 13, respectively.

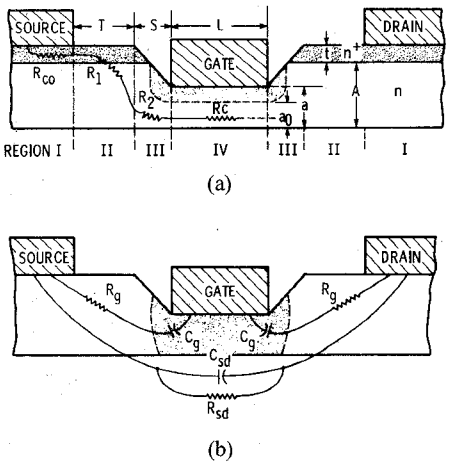

Fig. 14. Schematic cross section of a GaAs MESFET illustrating various resistive and capacitive regions. (a) ON state. (b) OFF state.

VI. Design Considerations for an Optically Controlled Depletion-Mode MESFET Switch

When no gate bias is applied to the MESFET, it is said to be in the ON state. The ON-state resistance of the MESFET is a series combination of the drain and source contact resistance R_{co}, the gate-to-source and drain-to-gate parasitic resistance, and the channel resistance R_c. These resistances are shown in Fig. 14(a) and the following closed-form expressions can be used for calculating their values [23], [24]

$$R_{co} = \frac{2.1}{Wtn_+^{0.66}}\Omega \tag{14}$$

$$R_1 = \frac{1.1T}{Wtn_+^{0.82}} + \frac{1.1}{Wn^{0.82}}\left(\frac{A-a}{a}\right)^{0.5}\Omega \tag{15}$$

$$R_2 = \frac{1.1(t+A-a)}{Wan^{0.82}}\Omega \tag{16}$$

$$R_c = \frac{1.1L}{Wa_0 n^{0.82}}\Omega \tag{17}$$

where

$$a_0 = \frac{0.378}{n^{0.5}}\left[(V_p+0.85)^{0.5} - (0.85)^{0.5}\right] \tag{18}$$

and W is the gate width in millimeters, t is the thickness of the $n+$ region below the source and drain contacts in μm, $n+$ is the doping density of the contact layer expressed in units of $10^{16}/\text{cm}^3$, A is the thickness of the active layer, and a is the thickness of the active layer below the recessed gate. The ON-state resistance is therefore

$$R_{ON} = R_c + 2(R_{co} + R_1 + R_2). \tag{19}$$

When a gate voltage V_{gs} is applied such that $|V_{gs}| > |V_p|$, the MESFET is said to be in the OFF state. The OFF-state impedance is a parallel combination of the source-to-drain fringing capacitance C_{sd}, drain-to-gate and gate-to-source capacitance C_g, charging resistor R_g, and loss resistance R_{sd}. The equivalent circuit is shown in Fig. 14(b). The source-to-drain capacitance is estimated to be about 0.14 pF from geometrical considerations [24]; C_g is computed using the closed-form expression [24]

$$C_g = 0.06\frac{WL}{a}\text{ pF} \tag{20}$$

where L is the gate length in μm. The resistances R_{sd} and R_g are estimated to be about 3 kΩ and one-half of R_{ON}, respectively [24]. Normally, in the OFF state, $1/\omega C_g R_g \gg 1$; hence, the effective drain-to-source capacitance is $C_{sd} + 0.5\,C_g$ and the effective OFF-state resistance is a parallel combination of R_{sd} and $1/2R_g\omega^2(0.5C_g + C_{sd})^2$. Table II presents the assumed and calculated physical, electrical, and optical parameters of the MESFET.

TABLE II
ON-State and OFF-State Equivalent Circuit Parameters for a Typical 1-μm GaAs MESFET Optical Switch

PHYSICAL PARAMETERS	ELECTRICAL PARAMETERS	OPTICAL PARAMETERS
W = 1000 μm	ON-STATE	λ = 0.87 μm
L = 1 μm	R_{co} = 0.22 Ω	P = 1 W/cm^2
A = 0.3 μm	R_1 = 0.28 Ω	α = 10^4/cm
T = 1.9 μm	R_2 = 0.41 Ω	τ = 1x10^{-8} sec
S = 0.285 μm	R_c = 3.48 Ω	V_{lit} = 0.9 V
t = 0.1 μm	R_{on} = 5.31 Ω	
a = 0.115 μm		
a_0 = 0.048 μm	OFF - STATE	
n_+ = 1x10^{19}/cm^3	R_g = 2.65 Ω	
n = 1x10^{17}/cm^3	R_{sd} = 3 kΩ	
V_p = -0.9 V	C_g = 0.52 pF	
ϵ_r = 13.1	C_{sd} = 0.14 pF	
	EFFECTIVE R_{off} = 2.4 KΩ AT 10 GHz	

The pinchoff voltage and the light-induced voltage computed using (2) and (5) are -0.9 V and $+0.9$ V, respectively, for the above MESFET. Hence, a voltage equal to -0.9 V pinches off the channel and turns the MESFET off. By illuminating the MESFET, a voltage equal to $+0.9$ V is generated at the Schottky gate which overcomes the pinchoff voltage and turns the MESFET on.

The figure of merit of a MESFET switch is defined as the ratio of the effective OFF-state resistance to the ON-state resistance. For the MESFET switch under consideration, the figure of merit is about 450 at 10 GHz, which is considered to be a good figure since it translates to an insertion loss of 0.50 dB and an isolation greater than 25 dB for a single SPST switch [25].

VII. Effect of Illumination on f_T and f_{max}

The gate-to-source capacitance C_{gs} increases with illumination by as much as 28 percent [5], [21]. The increase in C_{gs} tends to lower the unity current gain frequency f_T and the unity maximum available gain frequency f_{max}.

VIII. Conclusions

The computed results show that the $Al_{0.3}Ga_{0.7}As/GaAs$ HEMT has the highest sensitivity to optical illumination of photon energy greater than the semiconductor band gap. Besides, numerical computations show that the channel conductance and also the gate-to-source capacitance increase, and the switching time decreases, with optical

illumination. Further, the transconductance is insensitive to optical illumination. Lastly, the design considerations are presented for realizing an optically switchable GaAs MESFET SPST switch with insertion loss of about 0.50 dB and isolation greater than 25 dB at 10 GHz.

REFERENCES

[1] R. G. Hunsperger, "Optical control of microwave devices," in *Integrated Optical Circuit Engineering II*, SPIE vol. 578, S. Sriram, Ed. Bellingham: SPIE, 1985, pp. 40–45.

[2] J. Austin and J. R. Forrest, "Design concepts for active phased-array modules," *IEE Proc. F. Commun., Radar Signal Processing*, vol. 127, pp. 290–300, 1980.

[3] B. Monemar, K. K. Shih, and G. D. Petit, "Some optical properties of the $Al_xGa_{1-x}As$ alloy system," *J. Appl. Phys.*, vol. 47, pp. 2604–2613, 1976.

[4] K. B. Bhasin, G. E. Ponchak, and T. J. Kascak, "Monolithic optical integrated control circuitry for GaAs MMIC-based phased arrays," NASA, TM-87183, 1985.

[5] H. J. Sun, R. J. Gutmann, and J. M. Borrego, "Photo effects in common-source and common-drain microwave GaAs MESFET oscillators," *Solid-State Electron.*, vol. 24, pp. 935–940, 1981.

[6] H. Mizuno, "Microwave characteristics of an optically controlled GaAs MESFET," *IEEE Trans. Microwave Theory Tech.*, vol. MTT-31, pp. 596–600, 1983.

[7] A. A. A. DeSalles, "Optical control of GaAs MESFET's," *IEEE Trans. Microwave Theory Tech.*, vol. MTT-31, pp. 812–820, 1983.

[8] J. L. Gautier, D. Pasquet, and P. Pouvil, "Optical effects on the static and dynamic characteristics of a GaAs MESFET," *IEEE Trans. Microwave Theory Tech.*, vol. MTT-33, pp. 819–822, 1985.

[9] J. J. Pan, "GaAs MESFET for high-speed optical detection," in *Laser and Fiber Optics Communications*, SPIE vol. 150, M. Ross, Ed. Bellingham: SPIE, 1978, pp. 175–184.

[10] M. Yust *et al.*, "A monolithically integrated optical repeater," *Appl. Phys. Lett.*, vol. 35, pp. 795–797, 1979.

[11] F. J. Moncrief, "LEDs replace varactors for tuning GaAs FETs," *Microwaves*, vol. 18, no. 1, pp. 12–13, 1979.

[12] J. C. Gammel and J. M. Ballantyne, "An integrated photoconductive detector and waveguide structure," *Appl. Phys. Lett.*, vol. 36, pp. 149–151, 1980.

[13] S. M. Sze, *Physics of Semiconductor Devices*, 2nd ed. New York: Wiley, 1981.

[14] G. J. Chaturvedi, R. K. Purohit, and B. L. Sharma, "Optical effect on GaAs MESFETs," *Infrared Phys.*, vol. 23, pp. 65–68, 1983.

[15] M. S. Shur and L. F. Eastman, "Current-voltage characteristics, small-signal parameters, switching times and power–delay products of GaAs MESFET's," in *IEEE MTT-S Int. Microwave Symp. Dig.*, 1978, pp. 150–152.

[16] M. S. Shur, "Analytical model of GaAs MESFET's," *IEEE Trans. Electron Devices*, vol. ED-25, pp. 612–618, 1978.

[17] M. T. Abuelma'atti, "Modeling dc characteristics of HEMTs," *Electron. Lett.*, vol. 21, pp. 69–70, 1985.

[18] K. L. Chopra, S. Major, and D. K. Pandya, "Transparent conductors—A status review, *Thin Solid Films*, vol. 102, pp. 1–46, 1983.

[19] D. G. Parker, "Use of transparent indium tin oxide to form a highly efficient 20 GHz Schottky barrier photodiode," *Electron Lett.*, vol. 21, p. 778, 1985.

[20] A. A. DeSalles and J. R. Forrest, "Theory and experiment for the GaAs MESFET under optical illumination," in *Proc. 11th European Microwave Conf. Dig.*, 1981, pp. 280–285.

[21] H. J. Sun, R. J. Gutmann, and J. M. Borrego, "Optical tuning in GaAs MESFET oscillators," in *1981 IEEE MTT-S Int. Microwave Symp. Dig.*, pp. 40–42.

[22] H. Goronkin, M. S. Birrittella, W. C. Seelbach, and R. L. Vaitkus, "Backgating and light sensitivity in ion-implanted GaAs integrated circuits," *IEEE Trans. Electron Devices*, vol. ED-29, pp. 845–850, 1982.

[23] H. Fukui, "Determination of the basic device parameters of a GaAs MESFET," *Bell Syst. Tech. J.*, vol. 58, pp. 771–797, 1979.

[24] Y. Ayasli, "Microwave switching with GaAs FETs," *Microwave J.*, vol. 25, pp. 61–74, Nov. 1982.

[25] J. F. White, *Microwave Semiconductor Engineering*. New York: Van Nostrand Reinhold, 1982, p. 147.

Rainee N. Simons (S'76–M'80) received the B.E. degree in electronics and communications from the Mysore University in 1972, the M.Tech. degree in electronics and communications from the Indian Institute of Technology, Kharagpur, in 1974, and the Ph.D. degree in electrical engineering from the Indian Institute of Technology, New Delhi, in 1983. His Ph.D. thesis investigated the propagation characteristics of slot line, coplanar waveguide and also finline at millimeter-wave frequencies.

He served as a lecturer in the department of electrical engineering, R. V. College of Engineering, Bangalore, during the academic year 1974–75. In addition, he served as a Senior Scientific Officer-II/I in the Center for Applied Research in Electronics (CARE) at IIT New Delhi from 1979–85. At CARE IIT New Delhi, he worked on millimeter-wave finline components and also toroidal latching ferrite phase shifters for phased arrays. Since 1985, he has been working as a National Research Council Resident Research Associate in the Solid State Technology Branch of the Lewis Research Center of the National Aeronautics and Space Administration (NASA) in Cleveland, OH. His current research interest is in the analysis and modeling of GaAs millimeter-wave semiconductor devices in MMIC's and in the direct optical control of MMIC modules in phased arrays.

Dr. Simons held the post of IEEE Student Chapter Chairman at IIT New Delhi from 1978–79. He also held the post of IEEE India Council ED/MTT Society Chapter (New Delhi) Joint Secretary, Executive Committee Member, and Vice Chairman during the years 1982, 1983, and 1984, respectively.

Kul B. Bhasin (S'74–M'83) received the Ph.D. degree in experimental solid-state physics from the University of Missouri-Rolla in 1976. His M.S., in the same field, was conferred in 1972 by Purdue University.

He is currently a member of the solid-state technology branch of the Space Communications Division, NASA Lewis Research Center, Cleveland, OH. Prior to joining NASA in 1985, he was Research Associate Professor of electrical engineering at the University of Cincinnati, and Research Associate at NASA-LRC. From 1977 to 1983, he was employed by Gould, Inc., as Manager of Technology.

Dr. Bhasin recently coedited the book *Microwave Integrated Circuits* (Artech House). He is a past recipient of the Gould Scientific Achievement Award. His affiliations include APS, AVS, and Sigma Xi. Current research activities include the areas of microwave and optical devices and integrated circuits for space communication applications.